Schottky forward current transport mechanisms in AlGaN/GaN HEMTs over a wide temperature range*

Wu Mei(武 玫)[a)b)], Zheng Da-Yong(郑大勇)[c)], Wang Yuan(王 媛)[b)], Chen Wei-Wei(陈伟伟)[b)], Zhang Kai(张 凯)[a)b)], Ma Xiao-Hua(马晓华)[b)], Zhang Jin-Cheng(张进成)[a)b)], and Hao Yue(郝 跃)[a)b)†]

[a)] *School of Microelectronics, Xidian University, Xi'an* 710071, *China*

[b)] *Key Laboratory for Wide Band-Gap Semiconductor Materials and Devices, School of Microelectronics, Xidian University, Xi'an* 710071, *China*

[c)] *The Fifth Electronics Research Institute of Ministry of Industry and Information Technology, Guangzhou* 510610, *China*

(Received 18 March 2014; revised manuscript received 8 April 2014; published online 16 July 2014)

The behavior of Schottky contacts in AlGaN/GaN high electron mobility transistors (HEMTs) is investigated by temperature-dependent current–voltage (T–I–V) measurements from 300 K to 473 K. The ideality factor and barrier height determined based on the thermionic emission (TE) theory are found to be strong functions of temperature, while present a great deviation from the theoretical value, which can be expounded by the barrier height inhomogeneities. In order to determine the forward current transport mechanisms, the experimental data are analyzed using numerical fitting method, considering the temperature-dependent series resistance. It is observed that the current flow at room temperature can be attributed to the tunneling mechanism, while thermionic emission current gains a growing proportion with an increase in temperature. Finally, the effective barrier height is derived based on the extracted thermionic emission component, and an evaluation of the density of dislocations is made from the I–V characteristics, giving a value of 1.49×10^7 cm^{-2}.

Keywords: AlGaN/GaN HEMTs, Schottky contacts, forward current transport mechanism, temperature dependence

PACS: 73.61.Ey, 07.20.Dt, 85.30.Hi **DOI:** 10.1088/1674-1056/23/9/097307

1. Introduction

Due to numerous excellent physical properties of GaN such as wide band gap, large breakdown electrical field, and high electron saturation velocity, AlGaN/GaN HEMTs have gained extensive attention in the application for high temperature, microwave, and high power fields during the past few decades. Although significant improvement in the characteristics of AlGaN/GaN HEMTs has been realized, fabricating high-quality Schottky contacts still remains a challenge for the further enhancement of the device performance.

So far, extensive research has been made on the Schottky contacts in AlGaN/GaN HEMTs, most of which put their focus on the reverse leakage current. Yan *et al.*[1] found that the Frenkel–Poole (FP) emission dominates the reverse gate leakage current of AlGaN/GaN HEMTs on sapphire. Comparing the current transport mechanisms between AlGaN/GaN HEMTs and AlInN/GaN HEMTs, Turuvekerede *et al.*[2] considered that TE and FP emissions are the major mechanisms in AlGaN/GaN HEMTs, while the Fowler–Nordheim (FN) tunneling could not be neglected in the latter. Nevertheless, little attention has been paid to the forward characteristics which is equal in importance.

In this paper, a systematic study of the Schottky contacts characteristics in AlGaN/GaN HEMTs is presented by performing temperature-dependent current–voltage (T–I–V) measurements. We fit the experimental data with various current transport mechanisms, and demonstrate that the tunneling current is the main conduction mechanism at low bias throughout the entire measured temperature, while the TE component coincides with the experimental data only at higher bias. The temperature dependence of the accurate barrier height is also obtained. Besides, an estimation of the density of dislocations is made by using the extracted tunneling component.

2. Devices and experiments

The sample employed in this study is conventional Schottky contacts in AlGaN/GaN HEMTs grown by metal-organic chemical vapor deposition (MOCVD) on (0001) sapphire substrate. The epitaxial structure included an AlN nuclear layer, an unintentionally doped GaN layer of 1.2 μm thickness, an AlN interlayer of 1 nm thickness, and an AlGaN barrier layer of 20 nm. The sample was capped with a 1-nm-thick GaN layer. The measured room-temperature Hall mobility and sheet carrier density are 1418 cm^2/Vs and 1.2×10^{13} cm^{-2}, respectively. The sheet resistance of 360 Ω/sq was also obtained. The device fabrication started with mesa isolation performed by reactive ion etching (RIE) with an etching depth of 150 nm. The Ti/Al/Ni/Au (22 nm/140 nm/55 nm/45 nm)

*Project supported by the National Natural Science Foundation of China (Grant No. 61334002) and the Opening Project of Science and Technology on Reliability Physics and Application Technology of Electronic Component Laboratory of China (Grant No. ZHD201206).

†Corresponding author. E-mail: yhao@xidian.edu.cn

© 2014 Chinese Physical Society and IOP Publishing Ltd

metal stack was annealed in a nitrogen ambient at 850 °C for 30 s, resulting in an ohmic contact resistance of 0.8 Ω·mm. This is followed by the surface passivation of 60-nm Si_3N_4 dielectric by the plasma-enhanced chemical vapor deposition (PECVD). The Ni/Au/Ni (45 nm/200 nm/20 nm) metal stack was evaporated as Schottky contacts following the removel of Si_3N_4 under the gate using CF_4-based plasma. Finally, a 200-nm-thick Si_3N_4 was deposited as a second surface passivation film.

The temperature-dependent Schottky *I*–*V* characteristics were measured by an Agilent B1500A semiconductor parameter analyzer at seven different temperatures ranging from 300 K to 473 K. The sample temperature was controlled by the Westbond-K1200D digital temperature controller.

3. Results and discussion

As plotted in Fig. 1, the forward *I*–*V* characteristics of the Schottky contacts present a temperature-dependent trend in the measured bias range from room temperature to 473 K. At low bias, the current increases exponentially with voltage at each temperature. While the change of current with the applied voltage becomes gentle and tends to saturate gradually at higher bias, the primary reason of which may be the substantial voltage drop across the Schottky series resistance. It should be noted that with increasing temperature, the current increases significantly, a severe problem in their high-temperature applications.

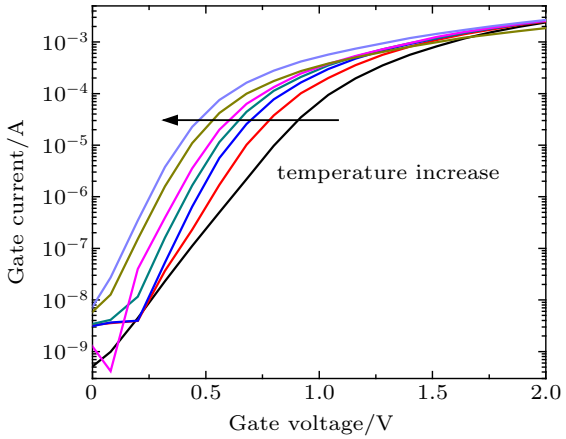


Fig. 1. (color online) Schottky forward characteristics of AlGaN/GaN HEMTs measured at various temperatures from 300 K to 473 K.

In general, the traditional TE theory is applied to illustrate the Schottky current transport characteristics, which can be expressed by

$$I = I_0 \exp\left\{\left[\frac{q(V - IR_s)}{nkT}\right] - 1\right\}, \tag{1}$$

$$I_0 = AA^*T^2 \exp\left(-\frac{q\varphi_B}{kT}\right), \tag{2}$$

where I_0 is the saturation current, A is the Schottky contact area, A^* is the effective Richardson constant, R_s is the Schottky series resistance, n and $q\varphi_B$ are the ideality factor and barrier height, respectively.

There are various methods for calculating the Schottky series resistance. Here the method developed by Cheung[3] is applied to extract this parameter. The following expression is obtained through a transformation of the forward *I*–*V* characteristics:

$$\frac{dV}{d\ln I} = R_s I + \frac{kT}{q}n. \tag{3}$$

Figure 2(a) shows the plot of $dV/d(\ln I)$ versus I at different temperatures, and hence, the R_s values can be obtained (see Fig. 2(b)). The extracted value of R_s increases from 231.8 Ω at room temperature to 319.7 Ω at 473 K, presenting a positive temperature coefficient. The result obtained by using this method is the total series resistance of the Schottky barrier diodes (SBDs), including the series resistance under the Schottky contacts, the series resistance between the ohmic contacts and the Schottky contacts, and the resistance of ohmic contacts which is insensitive to temperature.[4] Therefore, the increase in total series resistance with elevating temperature is mainly due to the decrease in the electron mobility. Moreover, the carriers will fill the traps in the bilateral materials during the heating process which may also has influence on it.

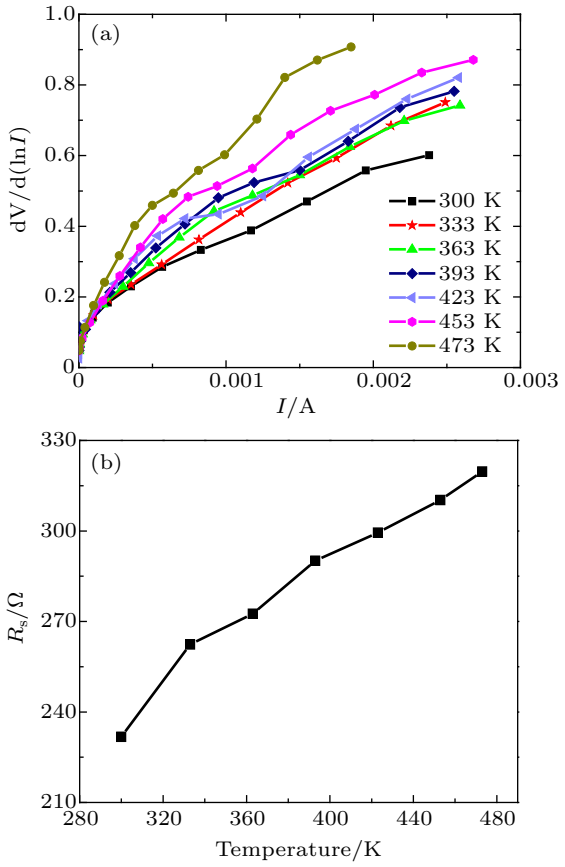


Fig. 2. (color online) (a) The $dV/d(\ln I)$ curves obtained from the forward *I*–*V* characteristics at various temperatures. (b) The temperature dependence of series resistance of the Schottky contacts in AlGaN/GaN HEMTs.

Assuming that the TE theory is the dominant mechanism throughout the applied bias, the ideality factor n and barrier height φ_B for each measured temperature can also be extracted as

$$n = \frac{q}{kT}\frac{\lg e}{\text{slope}}, \tag{4}$$

$$\varphi_B = \frac{1}{\lg e}\frac{kT}{q}\lg\frac{AA^*T^2}{\text{Intercept}}, \tag{5}$$

where slope and Intercept are extracted from the semi-logarithmic I–V characteristics. The resulting φ_B increases from 0.57 eV at room temperature to 0.82 eV at 473 K, whereas there is a corresponding monotonic decrease in the value of ideality factor n from 3.01 to 1.23. The conspicuous increase in the barrier height and the decrease in ideality factor with measurement temperature can be explained by the barrier height inhomogeneities. The ideal TE model regards n as nearly unity irrespective of temperature, which however, exhibits a great discrepancy from the experimental results, as shown in Fig. 3. However, the value of the ideality factor at room temperature is found to be far from unity, indicating that a single TE model is insufficient to explain the Schottky forward current characteristics, and that other mechanisms may also account for certain proportion in the process.

Thus, it is of great necessity to have a sound understanding of other models for an exhaustive explanation of the accurate current transport mechanisms of the SBDs. The other transport models involved mainly contain the recombination current I_{GR}, the tunneling current I_{TU}, and the edge leakage current I_{RL} associated with the surface leakage. It is necessary to assume that the ideality factor $n = 1$ in the TE model since the four mechanisms mentioned above are completely separated in the fitting procedure.

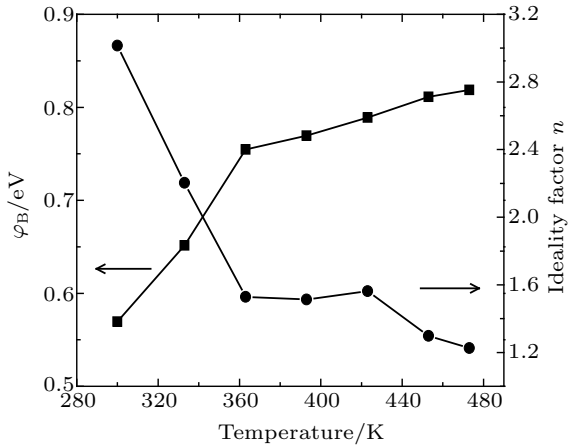


Fig. 3. The barrier height φ_B and the ideality factor n obtained at different temperatures from the TE model.

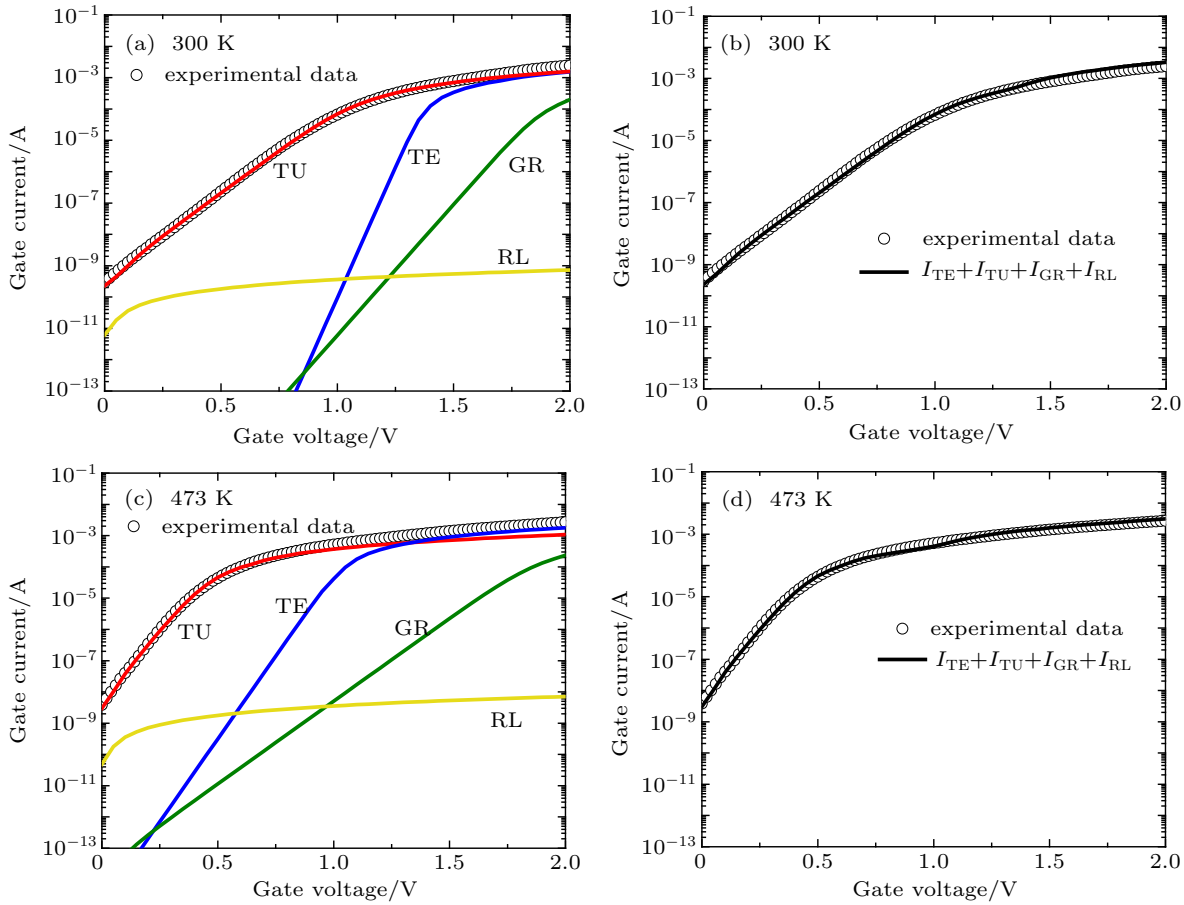


Fig. 4. (color online) Fitting results of the different mechanisms of the forward I–V characteristics at (a) room temperature and (c) 473 K, respectively. A comparison of the total simulation data and the experimental data at (b) room temperature and (d) 473 K, respectively.

The theory of recombination in SBDs is identical to that of p–n junctions, which is an alternative process for carriers to overcome the potential barrier in the space charge region, especially at lower temperature, which can be given by[5]

$$I_{\mathrm{GR}} = I_{\mathrm{GR}_0} \exp\left\{\left[\frac{q(V - IR_{\mathrm{s}})}{2kT}\right] - 1\right\}, \tag{6}$$

$$I_{\mathrm{GR}_0} = \frac{Aqn_{\mathrm{i}}W}{2\tau}, \tag{7}$$

where τ is the effective carrier life, W is the depletion width, and n_{i} is the intrinsic carrier concentration. In addition, the high density of trap states in the space charge region can assist carriers in tunneling into the semiconductor from metal, forming an important portion of the forward current. The corresponding tunneling current can be expressed as[6]

$$I_{\mathrm{TU}} = I_{\mathrm{TU}_0} \exp\left\{\left[\frac{q(V - IR_{\mathrm{s}})}{E_0}\right] - 1\right\}, \tag{8}$$

$$E_0 = E_{00} \coth\left(\frac{qE_{00}}{kT}\right), \tag{9}$$

where I_{TU_0} is the saturation tunneling current dependent on temperature, which is also related to barrier height and the parameters of semiconductor, and E_0 is the character energy. Beyond all that, the surface leakage component may become remarkable when the bias is low enough, that is[7]

$$I_{\mathrm{RL}} = \frac{V - IR_{\mathrm{s}}}{R_{\mathrm{L}}}, \tag{10}$$

where R_{L} is a shunt resistance mainly related to the ohmic contacts and surface leakage. According to the discussion above, finally, we obtain a complex model given by the following relationship:

$$I = I_0 \exp\left\{\left[\frac{q(V - IR_{\mathrm{s}})}{kT}\right] - 1\right\} + I_{\mathrm{GR}_0} \exp\left\{\left[\frac{q(V - IR_{\mathrm{s}})}{2kT}\right] - 1\right\} + I_{\mathrm{TU}_0} \exp\left\{\left[\frac{q(V - IR_{\mathrm{s}})}{E_0}\right] - 1\right\} + \frac{V - IR_{\mathrm{s}}}{R_{\mathrm{L}}}. \tag{11}$$

For a precise interpretation of the dominant transport process of the forward current in Ni/Au-AlGaN/GaN Schottky contacts, we fit the experimental data at different temperatures from 300 K to 473 K. Numerical simulation of each curve is made and compared to the experimental characteristics. Figure 4 shows the results at room temperature and 473 K, respectively. A good agreement with the experimental curve can be clearly observed.

As shown in Fig. 4, at room temperature, the tunneling component dominates almost the entire bias range of 0–2 V, whereas the thermionic emission current approaches the experimental data merely for voltage greater than 1.5 V. With increasing temperature, the thermionic emission current component plays an increasingly important role and, at 473 K, becomes the leading component when the bias is greater than 1 V. It should be noticed that the linear portion can still be well fitted by the tunneling mechanism. Besides, neither of the other two mechanisms is noticeable in our case. Since the current transport mechanism is anything but simplex, the traditional I–V method is no longer suitable for the extraction of the barrier height, and it is necessary to figure out the accurate barrier height through the extracted thermionic emission component. From Fig. 5, we can see that the barrier height decreases from 1.61 eV at room temperature to 1.43 eV at 473 K, presenting a negative temperature coefficient, which is possibly due to the thermally induced band gap shrinkage effect.

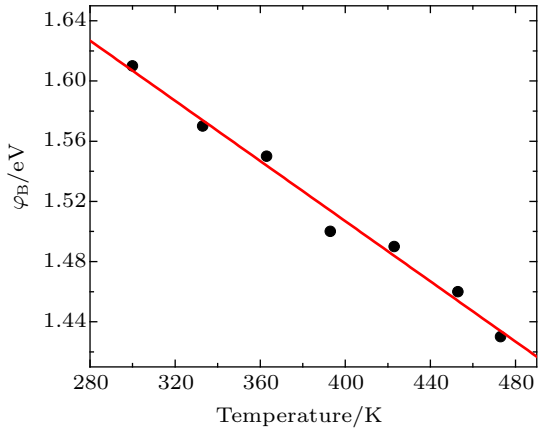


Fig. 5. (color online) Temperature-dependent characteristics of the barrier height based on the extracted thermionic emission current.

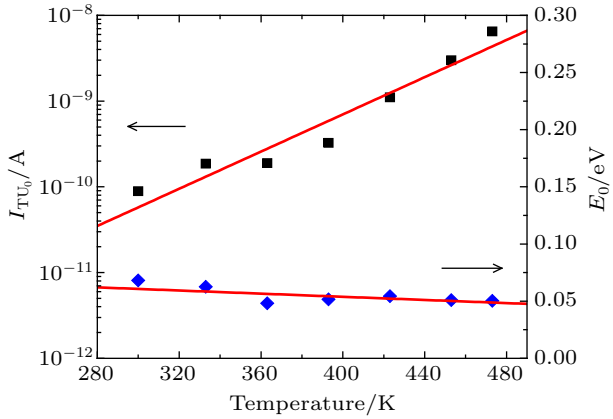


Fig. 6. (color online) Temperature dependence of the tunneling saturation current I_{TU_0} and the character energy E_0 calculated from the tunneling current component fits to the experimental data.

For a more detailed comprehension of the tunneling model, figure 6 presents a plot of I_{TU_0} and E_0 versus temperature from 300 K to 475 K, where the values of E_0 show a weak temperature dependence, the very property of the tunneling mechanism in AlGaN/GaN HEMTs with a high dislocation density.[9] Whereas I_{TU_0} changes exponentially with increasing temperature, which is different from the commonly reported results. Much stronger dependence of I_{TU_0} on temperature has also been reported by Donoval *et al.*[10] Furthermore, the density of dislocations can be obtained by using the known I_{TU_0} and E_0, expressed as[11]

$$D_{\mathrm{dis}} = \frac{I_{\mathrm{TU}_0}(0)}{qv_{\mathrm{D}}} \exp\left(\frac{\varphi_{\mathrm{B}}}{E_0(0)}\right), \tag{12}$$

where $D_{\rm dis}$ is the density of dislocations, $I_{\rm TU_0}(0)$ and $E_{\rm g}(0)$ can be determined by extrapolating the temperature dependence of $I_{\rm TU_0}$ and E_0 to 0 K, and $\nu_{\rm D}$ is the Debye frequency of 1.68×10^{13} S^{-1}.[11] The value of $\varphi_{\rm B}$ can be calculated from the dependence on the band gap $E_{\rm g}$ in GaN in view of the Fermi-level pinning effect, given by

$$\varphi_{\rm B} \cong \frac{1}{3}E_{\rm g}(0). \tag{13}$$

By substituting $I_{\rm TU_0}(0) = 1.29\times10^{-12}$ A, $E_0(0) = 0.071$ eV, and $E_{\rm g}(0) = 3.47$ eV into Eq. (12), the calculated density of dislocation is about 1.49×10^{7} cm^{-2}, which is in consistence with the reported data in the literatures.[12,13] This result may support the assumption that the tunneling mechanism governed by dislocations is the predominant current mechanism in Ni/Au AlGaN/GaN Schottky contacts as many researchers ascribed. However, the thin surface barrier (TSB) model was previously proposed by Hasegawa[8] in which the presence of the unintentional surface donors may reduce the width of the Schottky barrier so that carriers are able to tunnel the potential barrier easily. We have also found that the nitrogen vacancy at GaN surface induced during the process may be the origin of the surface donor states, which plays a pivotal role in the tunneling process.

4. Conclusions

The Schottky forward I–V characteristics of AlGaN/GaN HEMTs was investigated in the temperature range from room temperature to 473 K. It is observed that temperature has a great influence on the main parameters of the devices. The increase in the Schottky series resistance with rising temperature is mainly due to the reduction of carrier mobility at higher temperature. With the temperature-dependent series resistance taken into account, it is found that the traditional TE model cannot explain the current transport appropriately, only fitting the experimental data at higher bias, and that the predominant mechanism at room temperature is the tunneling component. The accurate barrier height is deduced based on the extracted thermionic current, which decreases from 1.61 eV at room temperature to 1.43 eV at 473 K, resulting from the band gap shrinkage effect.

References

[1] Yan D W, Lu H, Cao D S, Chen D J, Zhang R and Zheng Y D 2010 *Appl. Phys. Lett.* **97** 153503
[2] Turuvekere S, Karumuri N, Rahman A A, Bhattacharya A, DasGupta A and DasGupta N 2013 *IEEE Electron Dev. Lett.* **60** 3157
[3] Cheung S K and Cheung N W 1986 *Appl. Phys. Lett.* **49** 85
[4] Cao Z F, Lin Z J, Lü Y J, Luan C B, Yu Y X, Chen H and Wang Z G 2012 *Chin. Phys. B* **21** 017103
[5] Yu A Y C and Snow E H 1968 *J. Appl. Phys.* **39** 3008
[6] Donoval D, Barus M and Zdimal M 1991 *Solid-State Electron.* **34** 1365
[7] Kotani J, Tajima M, Kasai S and Hashizume T 2007 *Appl. Phys. Lett.* **91** 093501
[8] Hasegawa H and Susumu O 2002 *J. Vac. Sci. Technol. B* **20** 041647
[9] Estropov V V, Dzhumaeva M, Zhilyaev Y V, Nazarov N, Sitnikova A A and Fedorov L M 2000 *Semiconductors* **34** 1305
[10] Donoval D, Chvala A, Sramaty R, Kovac J, Morvan E, Dua Ch, Diforte-Poisson M A and Kordos P 2011 *J. Appl. Phys.* **109** 063711
[11] Arslan E, Altinadal S, Ozcelik S and Ozbay E 2009 *J. Appl. Phys.* **105** 023705
[12] Zhang A P, Rowland L B, Kaminsky E B, Tilak V, Grande J C, Teetsov J, Vertiatchikh A and Eastman L F 2003 *J. Electron. Mater.* **32** 388
[13] Lü Y J, Feng Z H, Lin Z J, Gu G D, Dun S B, Yin J Y, Han T T and Cai S J 2014 *Chin. Phys. B* **23** 027101